

ESS DTL: FINAL INSTALLATION AND FIRST COMMISSIONING RESULTS UP TO 74 MeV

F. Grespan^{†,1}, C. Baltador, L. Bellan, M. Comunian, M. Montis, A. Palmieri, A. Pisent
INFN-LNL, Legnaro, Italy

T. Bencivenga, P. Mereu, C. Mingioni, M. Nenni, E. Nicoletti, INFN-Torino, Torino, Italy

B. Jones, Y. Levinsen, R. Miyamoto, N. Milas, L. Page, C. Plostinar, R. Zeng, ESS, Lund, Sweden

¹also at ESS, Lund Sweden

Abstract

The Drift Tube Linac (DTL) for the European Spallation Source (ESS ERIC) will accelerate proton beam up to 62.5mA peak current from 3.62 to 90 MeV. The 5 cavities are now fully installed and tested in the linac tunnel. Moreover, in 2023 DTL1 to DTL4 have been RF conditioned to full power and beam commissioned with max peak current at short pulses. Relevant results of these activities are presented in this paper.

INTRODUCTION

Status of Installation.

A total of 5 cavities of the Drift Tube Linac (DTL5) for the European Spallation Source (ESS ERIC) were installed in September 2023 (Fig. 1), following completion of beam commissioning at 74 MeV [1]. Tests were undertaken for vacuum leaks, alignment, and the RF parameters were validated. The assembly of RF windows and power couplers was completed in May 2024, after the high-power tests reported in Ref. [2]. The DTL5 is now connected to the cooling skid and ready for a series of integrated tests scheduled before high power conditioning in November 2024.

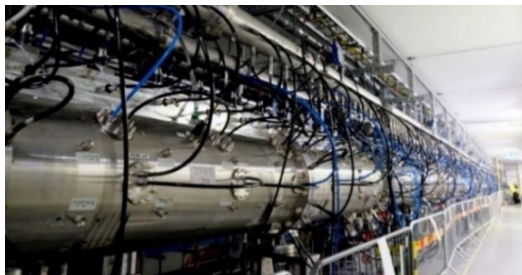


Figure 1: The 5 DTLs now installed in the ESS tunnel.

DTL5 comprises 23 cells, i.e., 22 drift tubes (DTs). The installation of DTs on the modules and module-to-module assembly follows the sequence described in Ref. [3]. Each assembly step is monitored with a laser tracker and leak tested. The total DT transverse errors specifications are ± 0.1 mm, and take into account the machining errors of DTs and girders, and the positioning errors of DTs in the modules, the PMQs inside DTs and module-module alignment. Transverse PMQ alignment is within specifications (± 0.1 mm) with the only exception of the high energy end plate. Longitudinally, the maximum gap-gap error is $< \pm 0.3$ mm, with the corresponding phase errors within the tolerance (< 0.5 deg). The process of tuning and stabilization

with Post Couplers (PCs) equipped with stubs is extensively described in Ref. [4]. The adjustable aluminium tuners and PCs are replaced with machined copper parts and cavity parameters are recorded (Table 1, Fig. 2).

Table 1: DTL5 RF Parameters (VNA Measurements)

| | Parameters | Design | Measured |
|------|---------------------------|---------|--|
| DTL5 | Freq. [MHz] | 352.21 | 352.266 (in vacuum, no RF power, 18°C) |
| | Coupl. factor [β] | 1.84 | 1.95 |
| | Q0 (SFish/1.25) | 43415 | 43307 |
| | E0 flatness [%] | ± 2 | ± 1.15 |
| | Tilt.Sens. | N.A. | ± 4.5 %/MHz |



Figure 2: E0, gap-gap phase error and DT transverse alignment of DTL5.

“As Built” Simulations

The data in Fig. 2, together with the data of DTL1-2-3-4 [5], are the inputs for the beam dynamics “as built” model. The simulation run with nominal current, 62.5 mA and nominal input beam rms emittances, 0.28/0.28/0.39 mm mrad. Steerers are activated to counteract PMQ misalignments, the max used steerer strength is 1 mT*m, with max possible strength 1.4 mT*m. The run is without losses with output emittances comparable with nominal case (Fig. 3).

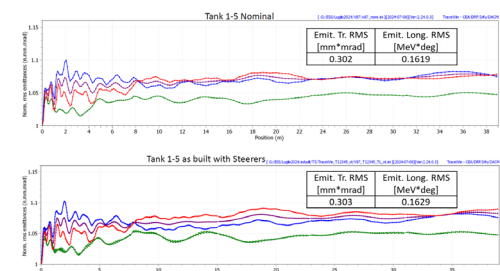


Figure 3: Nominal and “as built” DTL’s emittances.

CONDITIONING OF DTL1 TO 4

RF Conditioning Results

The high-power RF conditioning process aims to make the cavities ready to sustain beam operation, in terms of RF parameters (field, pulse length and repetition rate) and vacuum level. Conditioning of the DTLs starts at 10 μ s-10kW-1Hz. An automated conditioning routine is used. The routine consists in two cycling loops, the first ramping up the forward power (P_{FWD}) from 10 kW to the maximum allowed field E_0 , the second loop increase the pulse length once the power ramp restarts. Repetition rate is manually controlled. A plateau time is set at the end of each power ramp. The script reacts to interlocks (arc, cavity decay and vacuum) by decreasing power and pulse length until the levels return below a safety threshold. The 4 DTLs reached the nominal field and duty cycle ($P_{ave} \sim 60$ kW) in March 2023, including long stability run with more than 95% RF ON over 12 hours. Because of some multipacting activities on the windows of DTL2 and DTL3, further stability run has been repeated only for DTL1 and DTL4. To improve the vacuum conditions and mitigate the lightning, the o-ring seal between windows and coupler boxes has been replaced with a soft aluminium gasket [2].

Pick-up (p-up) Trends

Each DTL is equipped with 9 RF *p-ups* equally spaced, which can be used to monitor indirectly the field flatness, imposing the equivalence between the last bead pull measurement and *p-up* signal at low power. *P-up* #5 is the reference for LLRF loops. The *p-ups* of the DTLs are expected to have a calibration error bar of $\pm 5\%$, due to the method we use to determine the attenuation of the *p-up* $\alpha_{pu} = P_{p-up}/P_{cav} \sim -35$ dB. This error can be observed when comparing E_0 measured directly from the *p-up* attenuation with respect to E_0 expected from the cavity RF parameters reported in Table 1 for a given $P_{cav} = P_{FWD} - P_{REV}$ [5], being the second one more reliable because it is based on the more precise measurements of Q_0 . The calibration with beam will show similar results (see next section).

Looking more in detail at the signal of the 9 *p-ups* over the P_{ave} range [0.03-60] kW, we observed that all *p-ups* show a trend when changing the P_{ave} . The field flatness is perturbed as a function of P_{ave} (in Fig. 4 the DTL3 case). In absolute value, some *p-up* present larger variation, while others are more constant (Fig. 5).

What looks like a contradiction of the PCs resonant stabilization, it is in fact an effect of the stabilization itself. High-power operation induces thermal deformation of the DTs. These local perturbations excite the stabilization mechanism of the PCs, producing a detectable magnetic field at the *p-up* positions. These fields are superimposed on the TM_{010} magnetic field of the operating mode. This is a consequence of the resonant coupling stabilization, which, on the other hand, preserves the flatness on the axial accelerating field E_0 . COMSOL simulations have been performed to prove this effect: Figure 6 shows the results of introducing a ≈ 100 kHz perturbation on the high energy end cell of DTL3. The field flatness monitored at the *p-ups* reproduces

the measurements of Fig. 4, while the perturbation of E_0 is negligible. E_0 flatness preservation is confirmed by beam experiments described in the next section.

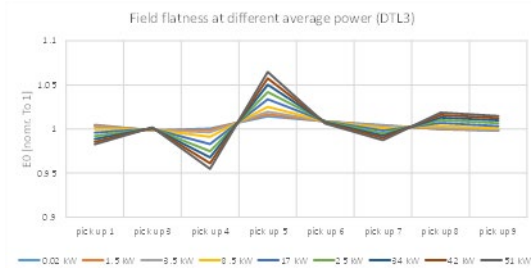


Figure 4: DTL3 field flatness for different P_{ave} .



Figure 4: DTL3 *p-up* trends for different P_{ave} .

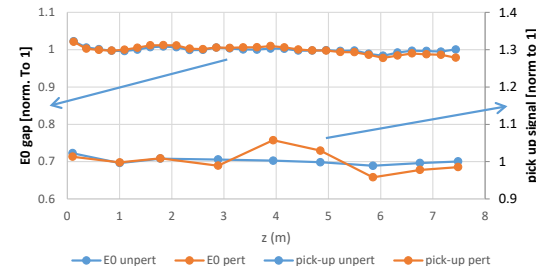


Figure 5: DTL3 E_0 gap field and *p-up* signal simulated with COMSOL, with and without perturbation.

BEAM EXPERIMENTS

RF Amplitude and Phase Tuning with Beam

The DTLs have internal BPMs: 6 in DTL1, 3 in DTL2 and 2 in DTL3-4-5. The correct amplitudes and phases are determined by phase scans at different amplitudes, then fitting the signals of the internal BPMs of the DTLs, induced by probe beam (5 mA, 5 μ s). The fitting algorithm, developed in PyORBIT, fits the data signal of the 1st and 2nd BPM with respect to a physical model to determine the correct RF amplitude and phase settings. All the DTLs have a 1st BPM after a few gaps, so that phasing is comparable with a single gap cavity. The RF amplitude can be fitted using only the 1st BPM. Nonetheless, the use of the 2nd BPM highly improves the matching with the model [6]. E_0 setpoints found by phase-scan are at $\pm 5\%$ with respect to the *p-up* value, which is consistent with the already mentioned calibration error (Table 2). $P_{cav}=P_{FWD}-P_{REV}$ at the new E_0 set points is much closer to the value expected by Q_0 measurements.

Table 2: E0 Set Points by Phase-scan of DTL1 to 4

| DTL | E0 MV/m | | P _{cav} kW | |
|-----|---------|-----------|---------------------|---------|
| | design | Set point | Set point | Expect. |
| 1 | 3.0 | 2.9 | 1160 | 1143 |
| 2 | 3.16 | 3.09 | 1310 | 1200 |
| 3 | 3.07 | 3.26 | 1082 | 1099 |
| 4 | 3.04 | 2.84 | 1140 | 1115 |

Longitudinal Acceptance of DTL1

The longitudinal acceptance area of DTL1 has been measured by recording the transmission as a function of the RF phase, injecting a pencil beam of 4 mA at 3 different input energies (3.4, 3.6 and 3.9 MeV), obtained with a proper setup of the 3 MEBT bunchers. The results are compared with simulations of the same pencil beam, starting from the plasma electrode of the ion source than transported through a realistic model of the LEBT. The RFQ is simulated at low current, and the output is then injected into the model of MEBT with buncher field maps, useful for TTF calculation for higher and lower energies than nominal. The beam is finally transported through the “as-built” model of DTL1. The results show a good agreement for all input energies, but we want to emphasize here that the lower energy probe beam supplies a benchmark for the field calibration. In fact, due to the shrinkage of the longitudinal acceptance at lower E0, the maximum transmission strongly depends on the field level (Fig. 7). Comparing with simulations, DTL1 field is compatible with an underestimation of the field of 5%, as already obtained from the phase scans.

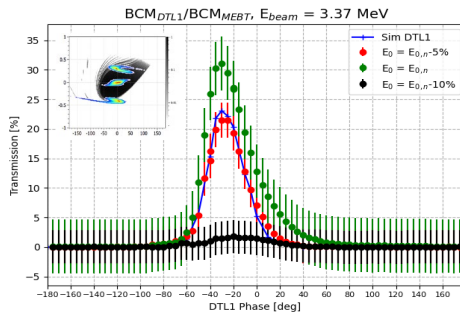


Figure 6: Measurement of DTL1 longitudinal acceptance at beam input energy 3.37 MeV.

Runs at Fixed Power and Fixed Field

To confirm that E0 flatness is preserved at different powers and that only the p-up signal is distorted by the PCs excitation, we compare transmissions and BPM phases at low-medium-high duty cycles, first running at fixed E0 and then running at fixed P_{FWD}. Figure 7 compares the beam phase difference (BPM2-BPM1) taken in DTL3 turned off and detuned, while scanning DTL2 RF phase. If the value of E0 is locked by LLRF loop, we observed significant differences with duty cycle. While, if P_{FWD} is kept constant, the beam phase figures coincide at different duty cycles. This effect is magnified far from the synchronous phase. The practical aspect of this is to choose as reference p-up the less perturbed by stabilization effects.

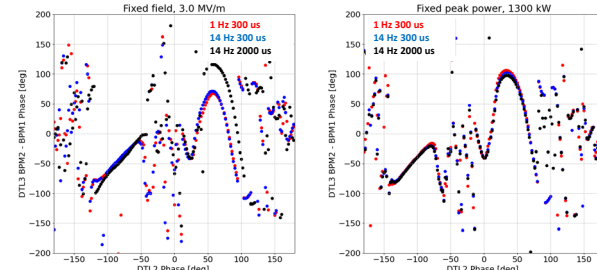


Figure 7: DTL3 BPM phase difference vs. DTL2 RF phase.

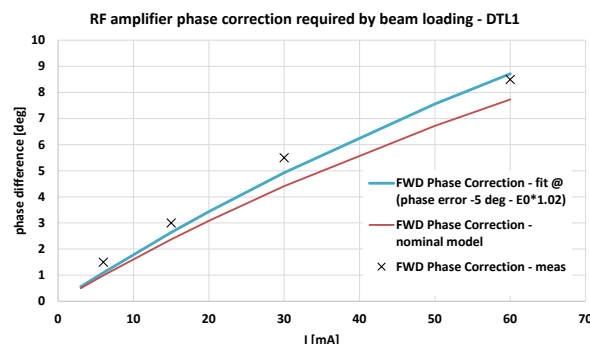
Beam Loading Approaches

The power delivered to the beam (P_{beam}) can be used as indicator of the RF set points. P_{beam} can be obtained from the sum of increased P_{FWD} and reduced P_{REV} over beam pulse. In this way, P_{beam} for all DTLs at 62.5 mA is obtained, and compared with the design P_{beam} (Table 3). This method does not immediately distinguish if the difference is due to field or phase setpoint. Nonetheless DTL2 and DTL3 show a discrepancy that should be investigated.

Table 3 Measured and Designed P_{beam} @ 62.5 mA

| | DTL1 | DTL2 | DTL3 | DTL4 |
|--------------------------|-------|------|-------|-------|
| P_{beam}^{meas} [kW] | 1113 | 1169 | 1075 | 1096 |
| P_{beam}^{design} [kW] | 1103 | 1113 | 1103 | 1103 |
| Difference [%] | +0.9% | +5% | -2.5% | -0.6% |

To discriminate between phase and field setpoint, we measured the P_{FWD} phase corrections required by beam loading in closed loop at different beam currents for DTL1 (Fig. 8). When compared to the model of a multicell accelerating cavity, the measured data can be better fitted with a reference phase 5 deg lower and E0 2% higher with respect to the set point. The use of beam loading based methods can be more extensively used besides phase scans in the upcoming commissioning phase.

Figure 8: P_{FWD} phase correction required by beam loading at different currents (DTL1).

CONCLUSIONS

As a summary, ESS DTLs is now installed and meet all specifications tested so far. We acknowledge of the excellent work done by the INFN and ESS technicians and ESS operators to support this work.

REFERENCES

[1] R. Miyamoto, “Status and plan of the European Spallation Source proton linac beam commissioning”, in *Proc. IPAC’23*, Venice, Italy, May 2023, pp. 2613-2616.
doi:10.18429/JACoW-IPAC2023-WE0GB1

[2] F. Grespan *et al.*, “RF and multipacting analysis of the high-power couplers of IFMIF/EVEDA RFQ and ESS DTLs”, presented at LINAC’24, Chicago, IL, USA, Sep. 2024, paper TUPB067, this conference

[3] F. Grespan *et al.*, “ESS Drift Tube linac manufacturing, assembly and tuning”, in *Proc. IPAC’21*, Campinas, Brazil, May 2021, pp. 1797-1800.
doi:10.18429/JACoW-IPAC2021-TUPAB173

[4] C. Baltador *et al.*, “Tuning of ESS DTLs” presented at LINAC’24, Chicago, IL, USA Sep. 2024, paper TUPB065, this conference.

[5] F. Grespan *et al.*, “Status and overview of the activities on ESS DTLs”, in *Proc. IPAC’23*, Venice, Italy, May 2023, pp. 851-854. doi:10.18429/JACoW-IPAC2023-MOPL127

[6] Y. Levinson *et al.*, “ESS normal conducting linac commissioning results”, in *Proc. HB’23*, Geneva, Switzerland, pp.118-122. doi:10.18429/JACoW-HB2023-TUA3I3